

https://dspace.org/

Closedform solutions for a reactiondiffussion sir model with different diffussion coeffecients

Rehana Naz; Andrew Gratien Johnpillai; Fazal Mahomed; Andrew Omame

https://hdl.handle.net/10539/46450
WOS

Downloaded from a DSpace repository. https://dspace.org/

Discrete & Continuous Dynamical Systems - Series S
Vol. 18, No. 4, April 2025, pp. 870-881
doi:10.3934/dcdss.2024103

CLOSED-FORM SOLUTIONS FOR A REACTION-DIFFUSION SIR MODEL WITH DIFFERENT DIFFUSION COEFFICIENTS

Rehana Naz[*1], Andrew Gratien Johnpillai[2], Fazal Mahmood Mahomed[3] and Andrew Omame[4]

[1]Department of Mathematics and Statistical Sciences, Lahore School of Economics, Lahore, 53200, Pakistan

[2]Department of Mathematics, Eastern University, Sri Lanka, 30350, Sri Lanka

[3]DDSI-NRF Centre of Excellence in Mathematical and Statistical Sciences University of the Witwatersrand, Johannesburg, Wits 2050, South Africa

[4]Department of Mathematics, Federal University of Technology, Owerri, Nigeria

Abstract. We use Lie point symmetries to obtain reductions and closed-form solutions for the reaction-diffusion SIR epidemic model. We determine that the Lie algebra for this model is three-dimensional. By invoking these Lie symmetries, we establish closed-form solutions for the reaction-diffusion SIR model. We employ the appropriate initial and boundary conditions to relate the derived closed-form solution to a real-world scenario. Furthermore, we utilize the closed-form solutions to generate a graphical representation of the densities of susceptible, infected, and removed individuals. We also perform a sensitivity analysis of the density of infected individuals to gain valuable insights into the transmission dynamics of the infectious disease.

1. **Introduction.** Researchers frequently employ the traditional SIR model as developed by Kermack-McKendrick [17] in their investigations and other adaptations of this model are also considered. Yang et al [34] investigated the traveling waves of a delayed SIR epidemic model with the same diffusion coefficients. Zhou et al [38] and Zhen et al [36] studied the traveling wave solutions and wave propagation of a delayed diffusive SIR epidemic model. Zhao [35] considered the two-group SIR epidemic model with constant recruitment. For the diffusive SIR model with nonlinear incidence, Wang et al [33] constructed the time periodic traveling waves. Later, Zhou et al [37] established the critical traveling waves for the same model. In [21], exact solutions of the diffusive SIR epidemic model [33, 37] for the same diffusion coefficients were established to study the transmission dynamics of COVID-19. In this paper, we study the reaction-diffusion SIR epidemic model with different diffusion coefficients [33, 37] for closed-form solutions from the Lie point symmetry perspective. Our study represents a novel exploration as, to the best of our knowledge, it has not been previously undertaken. Moreover, these solutions are employed to analyze the transmission dynamics of the infectious disease.

A literature survey shows that very few studies are reported up to now on the closed-form solutions of the epidemic model. Naz and Al-Raeei [19] developed a SIQD

2020 *Mathematics Subject Classification.* Primary: 22E70, 20C35; Secondary: 35Q92, 35C05.
Key words and phrases. Reaction-diffusion SIR epidemic model, symmetry approach.
*Corresponding author: Rehana Naz.

model for COVID and obtained the closed-form solutions using classical techniques of differential equations in order to understand the transmission dynamics of COVID 19. Nucci and Leach [26] looked at the singularity and symmetry of several epidemics models governed by ODEs to demonstrate the importance of the Lie group approach. In [25, 23, 24, 9, 10, 16], the Lie symmetry methods were employed to construct the first integrals and closed-form solutions of several epidemic models represented by ODEs. Prodanov [30] discussed the various analytical and numerical aspects of the SIR model. Kudryashov et al. [18] explored the analytical features of the SIR model, with a specific focus on its applications to COVID-19. The SIRD, SIRV, and other adaptations of the SIR model are also considered from the perspective of exact solutions and integrability [1, 2, 11]. The symmetry methods are successfully applied to the spatio-temporal epidemic models governed by PDEs [3, 8, 28] to derive the Lie symmetries and closed-form solutions.

Symmetry approach is an efficient tool that enables one to develop closed-form solutions of a given differential equation in a systematic manner. We refer the reader to some excellent books [4, 15, 27, 29] on the classical Lie symmetry method. The review article [20] includes details on various methods to generate the first integrals of ODEs, whereas the comparison between different ways of computing conservation laws for PDEs are presented in [22]. For the computation of Lie symmetries for differential equations, several efficient computer packages have been developed, see e.g. [6, 12, 31, 7, 13, 14]. In this work, we apply the classical Lie symmetry method (see, e.g. [4, 15, 27, 29]) for the SIR model. We find that the Lie algebra for this model is three-dimensional. We find a novel group invariant solution. The closed-form solution derived here is different from the traveling wave solutions derived by Wang et al [33] and Zhou et al [37].

The outline of the paper is as follows. In Section 2, the Lie point symmetries, reductions and closed-form solutions are obtained for the reaction-diffusion SIR epidemic model. We employ the appropriate initial and boundary conditions to relate the derived closed-form solution to a real-world scenario in Section 3. Moreover, we utilize the closed-form solutions to plot the densities of susceptible, infected, and removed individuals. We also perform a sensitivity analysis of the density of infected individuals to gain valuable insights into the transmission dynamics of the infectious disease. Finally, concluding remarks are provided in Section 4.

2. The Lie symmetries, reductions and closed-form solutions of a reaction-diffusion SIR epidemic model with different diffusion coefficient.

In this section, we will employ Lie symmetries to find reductions and closed-form solution for the reaction-diffusion SIR model.

2.1. The Lie symmetries of a reaction-diffusion SIR epidemic model with different diffusion coefficients.

Wang et al [33] considered the following reaction-diffusion SIR epidemic model

$$S_t = d_1 S_{xx} - \frac{\beta SI}{S+I}, \tag{1}$$

$$I_t = d_2 I_{xx} + \frac{\beta SI}{S+I} - \gamma I, \tag{2}$$

$$R_t = d_3 R_{xx} + \gamma I, \tag{3}$$

where $S(t,x), I(t,x)$ and $R(t,x)$ denote the densities of the susceptible, infected and removed individuals at time t and in location x, respectively. The parameter $\beta > 0$

denotes the infection rate, $\gamma > 0$ the recovery rate and d_i the diffusion coefficients. The variable $R(t,x)$ is not involved in the first two equations so we can consider the subsystem of equations (1) and (2). The fundamental reproduction number in the diffusion-free model, as stated by van den Driessche and Watmough [32], is represented as $\mathcal{R}_0$ and defined by the equation $\mathcal{R}_0 = \frac{\beta}{\gamma}$.

We provide a concise account on the Lie symmetry approach to the subsystem (1) and (2). Consider the vector field

$$X = \tau(t,x,I,S)\frac{\partial}{\partial t} + \xi(t,x,I,S)\frac{\partial}{\partial x} + \eta^1(t,x,I,S)\frac{\partial}{\partial I} + \eta^2(t,x,I,S)\frac{\partial}{\partial S}. \tag{4}$$

This operator X is a generator of a one-parameter Lie group of point transformations of the subsystem (1) and (2) if

$$\begin{aligned} X^{[2]}(S_t - d_1 S_{xx} + \frac{\beta SI}{S+I}) = 0, \\ X^{[2]}(I_t - d_2 I_{xx} - \frac{\beta SI}{S+I} + \gamma I) = 0, \end{aligned} \tag{5}$$

hold on the subsystem (1) and (2), where $X^{[2]}$ is the second prolongation of X, which can be easily deduced using known formulas from books [4, 15, 27, 29].

The determining equations for the functions τ, ξ, η^1 and η^2 yield the generators of point symmetries of the subsystem (1) and (2). Indeed by straightforward computations, the Lie point symmetries of the equations (1) and (2) are

$$\begin{aligned} X_1 &= \partial_t, \\ X_2 &= \partial_x, \\ X_3 &= S\partial_S + I\partial_I. \end{aligned} \tag{6}$$

One can utilize the computer programs, e.g. [6, 12, 31, 7] to establish these Lie point symmetries.

2.2. **Reductions using Lie symmetries X_1, X_2 and X_3.** The most general symmetry infinitesimal generator is

$$X = \partial_x + \mu\partial_t + \lambda(S\partial_S + I\partial_I). \tag{7}$$

Now, from the invariance surface conditions [4, 15, 27, 29], $X(S) = 0$ and $X(I) = 0$, we have:

$$\begin{aligned} S_x + \mu S_t = \lambda S, \\ I_x + \mu I_t = \lambda I. \end{aligned} \tag{8}$$

It is important to mention here that Lie symmetries enable reduction of the variable of the system of PDEs by one. Then the reduced system is easier to solve and in this case, we have the conditions as given in (8).

Equation (8) for $\mu \neq 0, \lambda \neq 0$ yields

$$\begin{aligned} S(t,x) &= F_1(\chi)e^{\frac{\lambda t}{\mu}}, \\ I(t,x) &= F_2(\chi)e^{\frac{\lambda t}{\mu}}, \end{aligned} \tag{9}$$

where $\chi = x - \frac{t}{\mu}$. With the aid of equation (9), the system of PDEs (1) and (2) reduces to the following system of ODEs:

$$\begin{aligned} F_1'' + \frac{F_1'}{\mu d_1} - \frac{\lambda F_1^2 + (\beta\mu + \lambda)F_1F_2}{\mu d_1(F_1 + F_2)} = 0, \\ F_2'' + \frac{F_2'}{\mu d_2} - \frac{(\gamma\mu + \lambda)F_2^2 + (\gamma\mu - \beta\mu + \lambda)F_1F_2}{\mu d_2(F_1 + F_2)} = 0, \end{aligned} \tag{10}$$

where the prime denotes differentiation with respect to the variable χ. While suitable mathematical software can be employed to establish numerical solutions of the system (10), this study primarily emphasizes deriving closed-form solutions.

2.3. **The closed-form solution of a reaction-diffusion SIR epidemic model.** If we insert $\mu = 0$, then equation (8) yields the following closed-form solution of system (1) and (2)

$$\begin{aligned} S(t,x) &= F_3(t)e^{\lambda x}, \\ I(t,x) &= F_4(t)e^{\lambda x}, \end{aligned} \tag{11}$$

and the system of PDEs (1) and (2) reduces to the following system of ODEs:

$$\begin{aligned} (F_3 + F_4)F_3' - d_1\lambda^2 F_3^2 - (\lambda^2 d_1 - \beta)F_3F_4 = 0, \\ (F_3 + F_4)F_4' + (\gamma - \lambda^2 d_2)F_4^2 + (-\lambda^2 d_2 - \beta + \gamma)F_3F_4 = 0. \end{aligned} \tag{12}$$

The solution of the reduced system of ODEs (12) for this case is

$$\begin{aligned} F_3(t) &= \Omega(t)e^{(\lambda^2 d_1 - \beta)t}, \\ F_4(t) &= -\Omega(t)\frac{A_2}{A_1}e^{(\lambda^2 d_2 - \gamma)t}, \end{aligned} \tag{13}$$

and

$$\Omega(t) = \left(\frac{A_2 - e^{-(\lambda^2 d_2 - \lambda^2 d_1 + \beta - \gamma)t}A_1}{\beta}\right)^{\frac{\beta}{\lambda^2 d_1 - \lambda^2 d_2 - \beta + \gamma}}, \tag{14}$$

where A_1 and A_2 are arbitrary constants of integration. The final form of the closed-form solution of the subsystem (1) and (2) using symmetries X_2 and X_3 is

$$\begin{aligned} S(t,x) &= \Omega(t)e^{(\lambda^2 d_1 - \beta)t + \lambda x}, \\ I(t,x) &= -\frac{A_2}{A_1}\Omega(t)e^{(\lambda^2 d_2 - \gamma)t + \lambda x}, \end{aligned} \tag{15}$$

where $\Omega(t)$ is given in (14). Substituting the expression for $I(t,x)$ from (15) into equation (3), the equation for R takes the following form

$$R_t = d_3 R_{xx} - \gamma\frac{A_2}{A_1}\Omega(t)e^{(\lambda^2 d_2 - \gamma)t + \lambda x}. \tag{16}$$

We have the well-known diffusion equation (see e.g. Cannon 1984 [5]) with source term. Thus, equation (16) is a linear inhomogeneous equation which have known solutions in the vast literature. It is known that by means of the superposition principle, the solution of the inhomogeneous equation is the sum of the solution of the homogeneous diffusion equation and a particular solution of the inhomogeneous equation. The closed-form solutions derived here are new and not reported before in the literature.

We have established the reductions and closed-form solutions for the reaction-diffusion SIR model. Using the combination of three Lie symmetries, X_1, X_2, and X_3, we reduced the subsystem of two second-order PDEs to a system of two second-order ODEs, which do not possess closed-form solutions. We established the closed-form

solution by utilizing Lie symmetries X_2 and X_3. By substituting the closed-form expression for $I(t,x)$ into the third equation of the reaction-diffusion SIR model, we obtained a diffusion equation for $R(t,x)$ with a time-dependent source term. This completes the Lie symmetry analysis, reductions, and closed-form solutions of the reaction-diffusion SIR system.

Remark 1. For the specific scenario of an infectious disease where the $R(t,x)$ compartment has a zero diffusion coefficient (i.e., $d_3 = 0$), the equation (16) for the density $R(t,x)$ of removed individuals yields:

$$R(t,x) = M(x) - \gamma \frac{A_2}{A_1} \int_0^t \left(\Omega(\tau) e^{(\lambda^2 d_2 - \gamma)\tau + \lambda x} \right) d\tau. \tag{17}$$

where $\Omega(\tau)$ is computed from (14) by setting $t = \tau$ and $M(x)$ is an arbitrary function of integration.

3. **The transmission dynamics of an infectious disease.** In this section, we employ the appropriate initial and boundary conditions. We study the relevance of derived closed-form solutions in a real-world scenario to understand transmission dynamics of an infectious disease with $d_3 = 0$. The resulting closed-form solution is visually depicted, considering specific parameter values derived from existing literature. Furthermore, we conduct a sensitivity analysis for three distinct scenarios, focusing on the epidemic peak and the implementation of control strategies.

3.1. **The utilization of initial and boundary conditions.** Let S_0, I_0 and R_0 denote the initial densities of susceptible, infected and removed individuals, respectively. Additionally, let $H(x)$ represents the initial distributions of the susceptible, infected and removed individuals across the spatial domain. Then, the initial conditions are defined as follows:

$$\begin{aligned} S(0,x) &= S_0 H(x),\ 0 \le x \le L, \\ I(0,x) &= I_0 H(x),\ 0 \le x \le L, \\ R(0,x) &= R_0 H(x),\ 0 \le x \le L. \end{aligned} \tag{18}$$

We consider time-dependent non-homogeneous Dirichlet boundary conditions at $x = 0$ and $x = L$:

$$\begin{aligned} S(t,0) &= G_1(t),\ 0 \le t \le T, \\ I(t,0) &= G_2(t),\ 0 \le t \le T, \\ R(t,0) &= G_3(t),\ 0 \le t \le T, \\ S(t,L) &= G_4(t),\ 0 \le t \le T, \\ I(t,L) &= G_5(t),\ 0 \le t \le T, \\ R(t,L) &= G_6(t),\ 0 \le t \le T. \end{aligned} \tag{19}$$

We utilize the initial conditions (18) for the group-invariant solution (11) which yields

$$F_3(0) = S_0,\ F_4(0) = I_0, \tag{20}$$

and the expression for $H(x)$

$$H(x) = e^{\lambda x}. \tag{21}$$

With the aid of (20), equations (13) and (14), yield the following values for A_1 and A_2

$$A_1 = -\frac{\beta S_0^{\frac{\lambda^2 d_1 - \lambda^2 d_2 + \gamma}{\beta}}}{S_0 + I_0}, \qquad A_2 = \frac{I_0}{S_0}\frac{\beta S_0^{\frac{\lambda^2 d_1 - \lambda^2 d_2 + \gamma}{\beta}}}{S_0 + I_0}. \tag{22}$$

We substitute the values of constants A_1 and A_2 from equation (22) into the expression for $\Omega(t)$ in equation (14) as well as into the closed-form solutions given by equations (15) and (17). The closed-form solution for variables $S(t,x)$, $I(t,x)$ and $R(t,x)$ can then be expressed as follows:

$$\begin{aligned} S(t,x) &= S_0\Theta(t)e^{(\lambda^2 d_1 - \beta)t + \lambda x}, \\ I(t,x) &= I_0\Theta(t)e^{(\lambda^2 d_2 - \gamma)t + \lambda x}, \\ R(t,x) &= R_0 e^{\lambda x} + \gamma I_0 \int_0^t \left(\Theta(\tau)e^{(\lambda^2 d_2 - \gamma)\tau + \lambda x}\right) d\tau, \end{aligned} \tag{23}$$

where $M(x) = R_0 e^{\lambda x}$ and the function $\Theta(t)$ is a known function of t given by

$$\Theta(t) = \left(\frac{I_0 + S_0 e^{-(\lambda^2 d_2 - \lambda^2 d_1 + \beta - \gamma)t}}{S_0 + I_0}\right)^{\frac{\beta}{\lambda^2 d_1 - \lambda^2 d_2 - \beta + \gamma}}, \tag{24}$$

and $\Theta(\tau)$ is computed from (24) by setting $t = \tau$.

Applying the time-dependent non-homogeneous Dirichlet boundary conditions (19) at $x = 0$ to equation (23) yields

$$\begin{aligned} G_1(t) &= S_0\Theta(t)e^{(\lambda^2 d_1 - \beta)t}, \\ G_2(t) &= I_0\Theta(t)e^{(\lambda^2 d_2 - \gamma)t}, \\ G_3(t) &= \gamma I_0 \int_0^t \left(\Theta(\tau)e^{(\lambda^2 d_2 - \gamma)\tau}\right) d\tau + R_0. \end{aligned} \tag{25}$$

Similarly, applying the time-dependent non-homogeneous Dirichlet boundary conditions (19) at $x = L$ to equation (23) yields

$$\begin{aligned} G_4(t) &= S_0\Theta(t)e^{(\lambda^2 d_1 - \beta)t + \lambda L}, \\ G_5(t) &= I_0\Theta(t)e^{(\lambda^2 d_2 - \gamma)t + \lambda L}, \\ G_6(t) &= \gamma I_0 \int_0^t \left(\Theta(\tau)e^{(\lambda^2 d_2 - \gamma)t + \lambda L}\right) d\tau + R_0 e^{\lambda L}. \end{aligned} \tag{26}$$

Consequently, the closed-form solution of the reaction-diffusion SIR model with the given initial conditions (18) and boundary conditions (19) is now fully established.

3.2. **Graphical representation of closed-form solutions.** The benchmark parameter values are assigned as follows: $S_0 = 10^6 - 200 - 50$, $I_0 = 200$, $R_0 = 50$, $\lambda = 1.0$, $d_1 = 0.2$, $d_2 = 0.3$, $\beta = 1.5$, and $\gamma = 0.5$. The reproduction number is $\mathcal{R}_0 = 3.0$. The time t is measured in days, x is measured in meters m, the diffusion coefficients d_1 for susceptible and d_2 for infected are measured in m^2/day, and the infection rate β and recovery rate γ are measured in day^{-1}. The closed-form solutions for the densities of the susceptible, infected and removed populations, given by equation (23), are graphically represented in Figure 1.

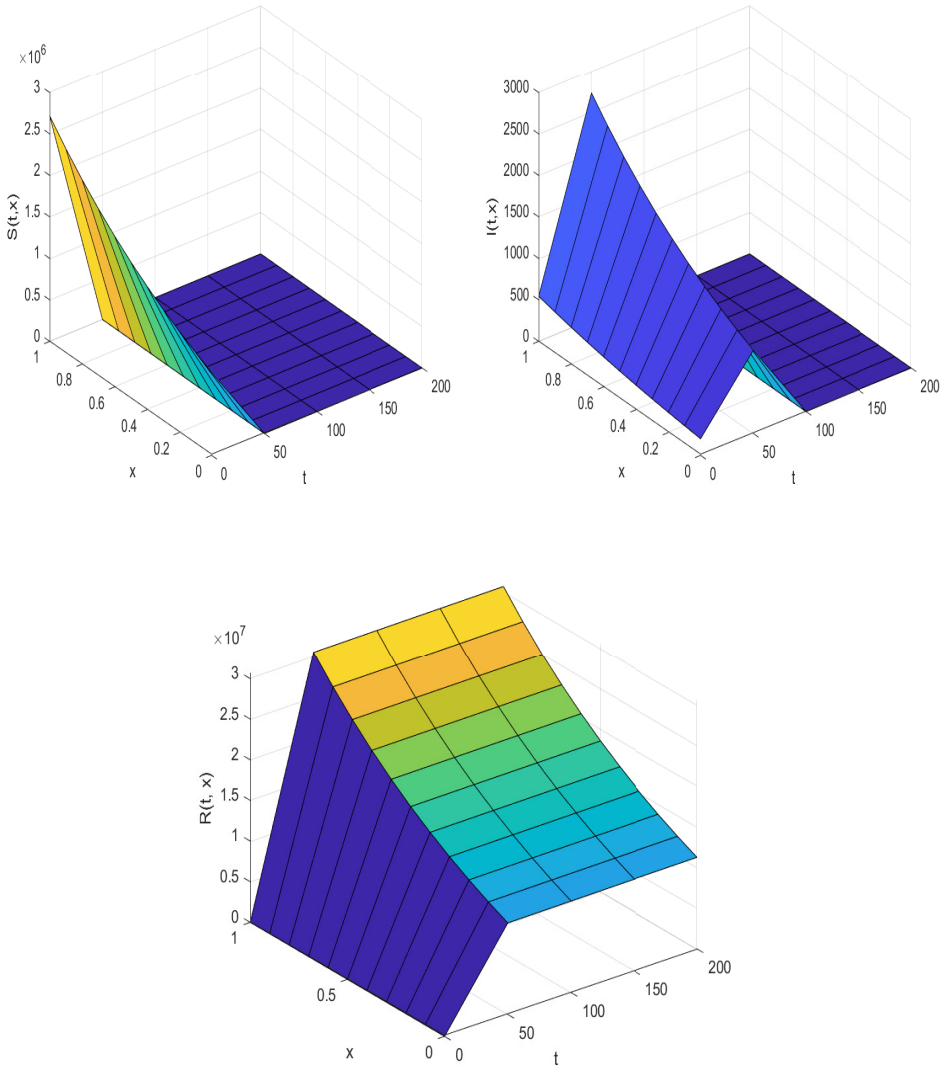


FIGURE 1. The surface plots for $S(t,x)$, $I(t,x)$ and $R(t,x)$ for $0 \leq t \leq 200$ and $0 \leq x \leq 1$. We used $S_0 = 10^6 - 200 - 50, I_0 = 200, R_0 = 50, \lambda = 1.0$, $d_1 = 0.2$, $d_2 = 0.3$, $\beta = 1.5$, $\gamma = 0.5$.

3.3. **Sensitivity analysis to understand transmission dynamics of an infectious disease.** We conduct a sensitivity analysis on the closed-form solution of the density of infected population, as provided in equation (23), considering three distinct scenarios. This analysis involves systematically varying the parameter values from their original benchmark values, which were employed to generate Figure 1. By varying the diffusion coefficient d_1 of the susceptible population, we investigate its impact on the epidemic peak. The graphical representation of this scenario is

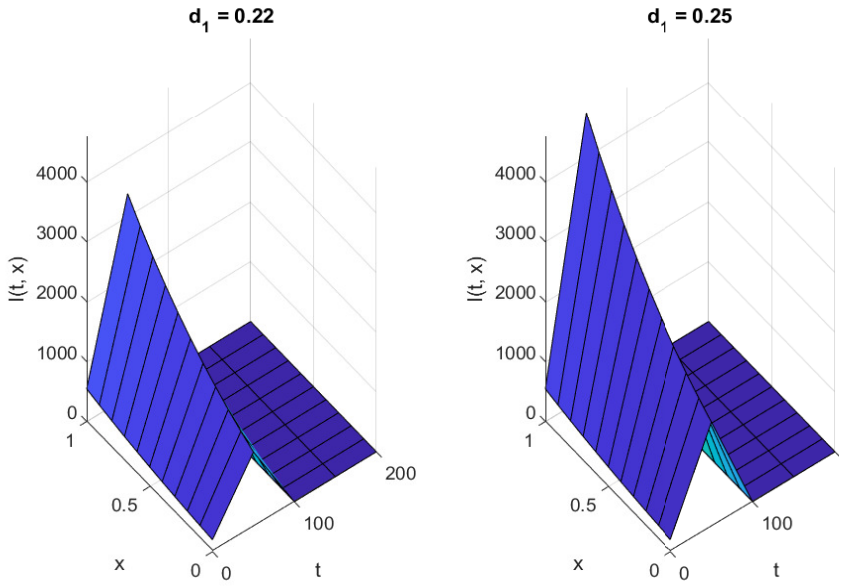


FIGURE 2. The effect of changing the diffusion coefficient d_1 of the infected population on the epidemic peak for $0 \leq t \leq 200$ and $0 \leq x \leq 1$. We used $S_0 = 10^6 - 200 - 50, I_0 = 200, R_0 = 50, \lambda = 1.0$, $d_2 = 0.3$, $\beta = 1.5$, $\gamma = 0.5$.

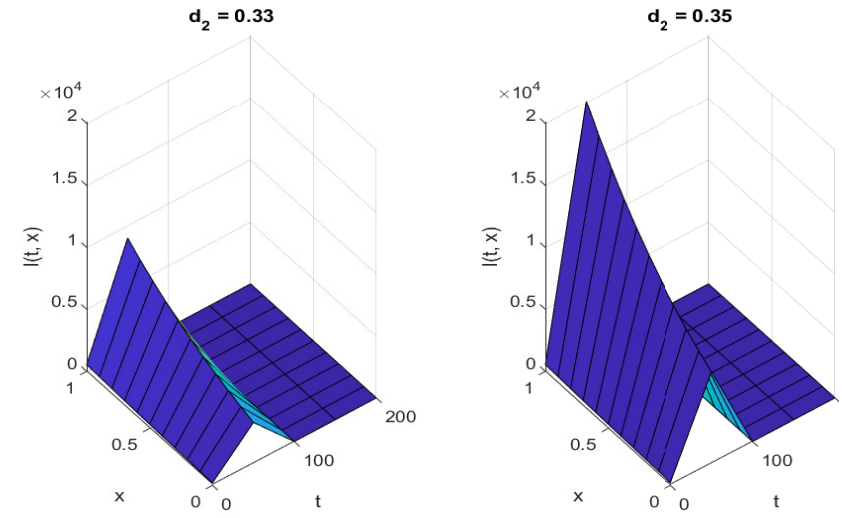


FIGURE 3. The effect of changing the diffusion coefficient d_2 of the infected population on the epidemic peak for $0 \leq t \leq 200$ and $0 \leq x \leq 1$. We used $S_0 = 10^6 - 200 - 50, I_0 = 200, R_0 = 50, \lambda = 1.0$, $d_1 = 0.2$, $\beta = 1.5$, $\gamma = 0.5$.

provided in Figure 2. In this case, the magnitude of the epidemic peak increases with higher values of the diffusion coefficient d_1.

In the second scenario, we analyze the effects on the epidemic peak by varying the diffusion coefficient d_2 of the density of infected population, while keeping other parameters fixed at benchmark values. This particular scenario is depicted graphically in Figure 3. Similar to the previous case, increasing the diffusion coefficient d_2 leads to an increase in the magnitude of the epidemic peak but for this case this is much higher than the scenario 1.

Based on these two scenarios, we can conclude that as the level of interaction among individuals rises, there is a corresponding increase in the number of infection cases. Therefore, in order to decrease the peaks of infection, it is necessary to intensify efforts aimed at reducing the mixing up of infected as well as susceptible individuals.

Figure 4 represents the effect of varying the γ, while keeping the other parameters fixed at the benchmark level. When we increase the recovery rate γ from 0.55 to 0.60 the corresponding value of reproduction number decreases from $\mathcal{R}_0 = 2.7273$ to $\mathcal{R}_0 = 2.5$. As a result, the infection peak is reduced, and the time required to reach such peaks is also shortened. Therefore, by decreasing the reproduction number through the implementation of enhanced treatment mechanisms for infected individuals, this measure will significantly mitigate the spread of the infection.

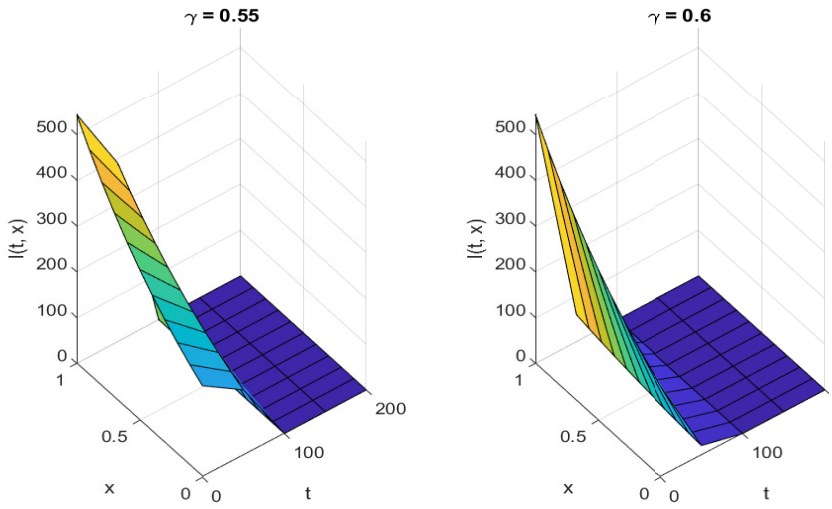


FIGURE 4. The effect of changing the recovery rate γ on the epidemic peak for $0 \leq t \leq 200$ and $0 \leq x \leq 1$. We used $S_0 = 10^6 - 200 - 50, I_0 = 200, R_0 = 50, \lambda = 1.0$, $d_1 = 0.2$, $d_2 = 0.3$, $\beta = 1.5$.

4. **Concluding remarks.** We have studied the reaction-diffusion SIR epidemic model with diffusion by utilizing the Lie symmetry approach for finding closed-form solutions. It was found that the underlying model admitted a three-dimensional Lie algebra. We utilized the most general Lie symmetry generator to reduce the system of PDEs to a system of two second-order ODEs. The combination of Lie symmetries X_2 and X_3 yielded the closed-form solutions for the reaction-diffusion SIR model. It is noteworthy to mention here that the symmetry approach for obtaining closed-form solutions for the epidemic model have not been reported in the previous literature. The results presented in this work are thus new and an extension of the studies on the epidemic model as elaborated in the Introduction.

We studied the relevance of derived closed-form solutions in a real-world scenario to understand transmission dynamics of an infectious disease with zero diffusion coefficient for the removed individuals. The appropriate initial and boundary conditions have been taken into account. The resulting closed-form solution was visually depicted, considering specific parameter values taken from existing literature. The density plots for susceptible, infected and removed populations were provided. Furthermore, a sensitivity analysis was conducted for three distinct scenarios, with a focus on the epidemic peak and the implementation of control strategies. By varying the diffusion coefficient of the susceptible population, we found that the magnitude of the epidemic peak increased with higher values of the diffusion coefficient. In the second scenario, we analyzed the effects on the epidemic peak by varying the diffusion coefficient of the density of infected population, while keeping other parameters fixed at benchmark values. We observed that increasing the diffusion coefficient led to a significantly higher magnitude of the epidemic peak compared to the first scenario. Based on these scenarios, we concluded that higher levels of interaction among individuals corresponded to increased infection cases. Therefore, to decrease infection peaks, efforts to reduce interaction between infected and susceptible individuals must be intensified. Lastly, when we increased the recovery rate γ while keeping the other parameters fixed at benchmark levels, the infection peak was reduced, and the time required to reach such peaks was shortened. Therefore, by decreasing the reproduction number through the implementation of enhanced treatment mechanisms for infected individuals, this measure significantly mitigated the spread of the infection.

Funding. This research received no external funding.

Competing interests. The authors have no relevant financial or non-financial interests to disclose.

Data availability. Data sharing not applicable to this article as no data sets were generated or analyzed during the current study.

REFERENCES

[1] N. A. Babaei, M. Kröger and T. Özer, Theoretical analysis of a SIRD model with constant amount of alive population and COVID-19 applications, *Appl. Math. Model*, **127** (2024), 237-258.

[2] N. A. Babaei and T. Özer, On exact integrability of a Covid-19 model: SIRV, *Math. Meth. Appl. Sci.*, **47** (2024), 3529-3546.

[3] F. Bacani, S. Dimas, I. L. Freire, N. A. Maidana and M. Torrisi, Mathematical modelling for the transmission of dengue: Symmetry and travelling wave analysis, *Nonl. Anal.: Real World Appl*, **41** (2018), 269-287.

[4] G. W. Bluman and S. Kumei, *Symmetries and Differential Equations*, Springer, New York, 1989.
[5] J. R. Cannon, *The One-Dimensional Heat Equation*, Encyclopaedia of Mathematics and its Applications, 1^{st} edition, Cambridge University Press, 1984.
[6] B. Champagne, W. Hereman and P. Winternitz, The computer calculation of Lie point symmetries of large systems of differential equations, *Comput. Phys. Commun.*, **66** (1991), 319-340.
[7] A. F. Cheviakov, GeM software package for computation of symmetries and conservation laws of differential equations, *Comput. Phy. Commun.*, **176** (2007), 48-61.
[8] I. L. Freire and M. Torrisi, Similarity solutions for systems arising from an Aedes aegypti model, *Commun. Nonl. Sci. Numer. Simul.*, **19** (2014), 872-879.
[9] B. U. Haq and I. Naeem, First integrals and exact solutions of some compartmental disease models, *Zeitschrift für Naturforschung A*, **74** (2019), 293-304.
[10] B. U. Haq and I. Naeem, First integrals and analytical solutions of some dynamical systems, *Nonl. Dyn*, **95** (2019), 1747-1765.
[11] T. Harko, F. S. N. Lobo and M. K. Mak, Exact analytical solutions of the Susceptible-Infected-Recovered (SIR) epidemic model and of the SIR model with equal death and birth rates, *Appl. Math. Comput.*, **236** (2014), 184-189.
[12] W. Hereman, SYMMGRP. MAX and other symbolic programs for Lie symmetry analysis of partial differential equation, *Lectures in Appl. Math*, **29** (1993), 241-257.
[13] W. Hereman, Symbolic software for Lie symmetry analysis, *CRC Handbook of Lie Group Analysis of Differential Equations*, **3** (1996), 367-413.
[14] W. Hereman, Review of symbolic software for Lie symmetry analysis, *Math. Comput. Model.*, **25** (1997), 115-132.
[15] N. H. Ibragimov, CRC handbook of Lie group analysis of differential equations, *CRC Press*, Boca Raton, FL, **1-3** (1994-1996).
[16] A. H. Kara, F. M. Mahomed, I. Naeem and C. Wafo Soh, Partial Noether operators and first integrals via partial lagrangians, *Math. Meth. Appl. Sci.*, **30** (2007), 2079-2089.
[17] W. O. Kermack and A. G. McKendrick, Contributions to the mathematical theory of epidemics, *Proc. Roy. Soc. London*, (1932).
[18] N. A. Kudryashov, M. A. Chmykhov and M. Vigdorowitsch, Analytical features of the SIR model and their applications to COVID-19, *Appl. Math. Model.*, **90** (2021), 466-473.
[19] R. Naz and M. Al-Raeei, Analysis of transmission dynamics of COVID-19 via closed-form solutions of a susceptible-infectious-quarantined-diseased model with a quarantine-adjusted incidence function, *Math. Meth. Appl. Sci.*, **44** (2021), 11196-11210.
[20] R. Naz, I. L. Freire and I. Naeem, Comparison of different approaches to construct first integrals for ordinary differential equations, *Abstr. Appl. Anal.*, (2014), 978636.
[21] R. Naz, A. G. Johnpillai and F. M. Mahomed, The exact solutions of a diffusive SIR model via symmetry groups, *J. Math. Forthcoming*.
[22] R. Naz, F. M. Mahomed and D. P. Mason, Comparison of different approaches to conservation laws for some partial differential equations in fluid mechanics, *Appl. Math. Comput.*, **205** (2008), 212-230.
[23] R. Naz, K. S. Mahomed and I. Naeem, First integrals and exact solutions of the SIRI and tuberculosis models, *Math. Meth. Appl. Sci.*, **39** (2016), 4654-4666.
[24] R. Naz and I. Naeem, The artificial Hamiltonian, first integrals, and closed-form solutions of dynamical systems for epidemics, *Zeitschrift für Naturforschung A*, **73** (2018), 323-330.
[25] R. Naz, I. Naeem and F. M. Mahomed, A partial Lagrangian approach to mathematical models of epidemiology, *Math. Prob. Engrg.*, (2015), Art. ID 602915, 11 pp.
[26] M. C. Nucci and P. G. L. Leach, Singularity and symmetry analyses of mathematical models of epidemics, *South African J. Sci.*, **105** (2009), 136-146.
[27] P. J. Olver, *Applications of Lie Groups to Differential Equations*, 2^{nd} edition, Springer-Verlag, New York, NY USA, 1993.
[28] Ö. Orhan, M. Torrisi and R. Tracinà, Group methods applied to a reaction-diffusion system generalizing Proteus Mirabilis models, *Commun. Nonl. Sci. Numer. Simul.*, **70** (2019), 223-233.
[29] L. V. Ovsiannikov, *Group Analysis of Differential Equations*, Academic Press, New York, 1982.
[30] D. Prodanov, Comments on some analytical and numerical aspects of the SIR model, *Appl. Math Model.*, **95** (2021), 236-243.

[31] T. M. Rocha Filho and A. Figueiredo, [SADE] a Maple package for the symmetry analysis of differential equations, *Comput. Phys. Commun.*, **182** (2011), 467-476.
[32] P. van den Driessche and J. Watmough, Reproduction numbers and sub-threshold endemic equilibria for compartmental models of disease transmission, *Math. Biosci.*, **180** (2002), 29-48.
[33] Z.-C. Wang, L. Zhang and X.-Q. Zhao, Time periodic traveling waves for a periodic and diffusive SIR epidemic model, *J. Dyn. Diff. Equ.*, **30** (2018), 379-403.
[34] J. Yang, S. Liang and Y. Zhang, Travelling waves of a delayed SIR epidemic model with nonlinear incidence rate and spatial diffusion, *Plos One*, **6** (2011), e21128.
[35] L. Zhao, Z.-C. Wang, and S. Ruan, Traveling wave solutions in a two-group SIR epidemic model with constant recruitment, *J. Math. Biol.*, **77** (2018), 1871-1915.
[36] Z. Zhen, J. Wei, L. Tian, J. Zhou and W. Chen, Wave propagation in a diffusive SIR epidemic model with spatio-temporal delay, *Math. Meth. Appl. Sci.*, **41** (2018), 7074-7098.
[37] J. Zhou, L. Song, J. Wei and H. Xu, Critical traveling waves in a diffusive disease model, *J. Math. Anal. Appl.*, **476** (2019), 522-538.
[38] K. Zhou, M. Han and Q. Wang, Traveling wave solutions for a delayed diffusive SIR epidemic model with nonlinear incidence rate and external supplies, *Math. Meth. Appl. Sci.*, **40** (2017), 2772-2783.

Received January 2024; revised June 2024; early access June 2024.